This document is the accepted manuscript version of the following article:
Schilling, I. E., Hess, R., Bolotin, J., Lal, R., Hofstetter, T. B., & Kohler, H. P. E. (2019). Kinetic isotope effects of the enzymatic transformation of γ-hexachlorocyclohexane by the lindane dehydrochlorinase variants LinA1 and LinA2. Environmental Science and Technology, 53(5), 2353-2363. https://doi.org/10.1021/acs.est.8b04234

Kinetic Isotope Effects of the Enzymatic Transformation of γ-Hexachlorocyclohexane by the Lindane Dehydrochlorinase Variants LinA1 and LinA2

Iris E. Schilling,[†,‡] Ramon Hess,[‡] Jakov Bolotin,[†] Rup Lal,[¶] Thomas B. Hofstetter,[†,‡] and Hans-Peter E. Kohler[*,†]

Eawag, Swiss Federal Institute of Aquatic Science and Technology, CH-8600 Dübendorf, Switzerland, Institute of Biogeochemistry and Pollutant Dynamics, ETH Zürich, CH-8092 Zürich, Switzerland, and Department of Zoology, University of Delhi, Delhi 110007, India

E-mail: hanspeter.kohler@eawag.ch

[*]To whom correspondence should be addressed
[†]Eawag
[‡]ETH Zürich
[¶]University of Delhi

Abstract

Compound-specific isotope analysis (CSIA) can provide insights into the natural attenuation processes of hexachlorocyclohexanes (HCHs), an important class of persistent organic pollutants. However, the interpretation of HCH stable isotope fractionation is conceptually challenging. HCHs exist as different conformers that can be converted into each other and the enzymes responsible for their transformation discriminate among those HCH conformers. Here, we investigated the enzyme-specificity of apparent ^{13}C- and ^{2}H-kinetic isotope effects (AKIEs) associated with the dehydrochlorination of γ-HCH (lindane) by two variants of the lindane dehydrochlorinases LinA1 and LinA2. While LinA1 and LinA2 attack γ-HCH at different *trans* 1,2-diaxial H–C–C–Cl moieties, the observed C and H isotope fractionation was large, typical for bimolecular eliminations, and not affected by conformational mobility. ^{13}C-AKIE-values for transformation by LinA1 and LinA2 were the same (1.024 ± 0.001 and 1.025 ± 0.001, respectively), whereas ^{2}H-AKIEs showed minor differences (2.4 ± 0.1 and 2.6 ± 0.1). Variations of isotope effects between LinA1 and LinA2 are small and in the range reported for different degree of C–H bond cleavage in transition states of dehydrochlorination reactions. The large C and H isotope fractionation reported here for experiments with pure enzymes contrasts previous observations from whole cell experiments and suggests that specific uptake processes by HCH-degrading microorganisms might modulate the observable HCH isotope fractionation at contaminated sites.

Introduction

Hexachlorocyclohexanes (HCHs) are members of the organochlorine group of insecticides and were extensively used in the past as insecticides in agriculture, forestry, and medicine. Technical HCH comprising a mixture of stereoisomers (i.e., α-, β-, γ-, δ-, and ϵ-HCH), whereby only the γ-isomer exhibited insecticidal activity, was widely used as a cheap but effective insecticide, especially in developing countries.[1] Later it was replaced by the pure γ-isomer (lindane), which was produced from technical HCH by fractional crystallization, a process that resulted in large amounts of isomeric waste.[2] Unfortunately, HCHs turned out to be persistent and toxic organic pollutants (POP)[3–5] and all isomers contribute in one way or another to today's environmental problems with HCHs.[6–8]

At contaminated sites, microbes have evolved that can use γ-HCH as a carbon and energy source under oxic conditions.[1,9,10] Aerobic biodegradation of γ-HCH, which is initiated by sequential dehydrochlorination and nucleophilic substitution reactions leading to less chlorinated cyclic hydrocarbons, is therefore rightly considered to be the basis for the development of bioremediation processes.[1] However, quantifying the extent of biodegradation after addition or stimulation of HCH degrading bacteria at contaminated sites and identifying the preferred routes of reaction are major challenges. On the one hand, competing abiotic processes, such as diffusion, sorption to the soil matrix and volatilization, which do not lead to an ultimate destruction of a contaminant, may be mistakenly taken for biodegradation. On the other hand, biodegradation may take place over timescales of decades[1] and its assessment based on interpretations of changes in concentrations will be difficult.

To overcome the limitations in assessing the progress of biodegradation, authors of recent studies proposed that progress of biodegradation of HCH isomers is best assessed through analysis of the changes of their $^{13}C/^{12}C$, $^{37}Cl/^{35}Cl$ and $^{2}H/^{1}H$ ratios at natural isotopic abundances.[11–18] Such compound-specific isotope analysis (CSIA) of HCHs is based on the assumption that stable isotope ratios of the remaining HCH change according to the kinetic isotope effects pertinent to the degradation reaction(s).[19–21] CSIA is well suited to study HCH biodegradation because an isotope

fractionation that would be indicative of the extent and the pathway(s) of transformation is independent of the timescale over which such transformations occur. Moreover, isotope fractionation for bond-cleavage reactions, such as dehydrochlorinations that initiate aerobic HCH biodegradation, are much more significant than would be expected for phase transfer processes.[20,22] Whereas CSIA has been frequently used to reveal natural attenuation of persistent chlorinated aromatic and olefinic chlorohydrocarbons,[23–26] its application to HCH isomers is still rather limited.[12,18,27] One reason is the high degree of chlorination that makes the conversion of HCH isomers to analyte gases for isotope ratio mass spectrometry more challenging so that procedures for measurement of $^{37}Cl/^{35}Cl$ and $^{2}H/^{1}H$ ratios have not been introduced until very recently.[28–31] Evaluation of HCH degradation by correlations of isotope fractionation from multiple elements is therefore almost unexplored.[32]

In addition to the above instrumental and analytical challenges, the interpretation of isotope fractionation of HCH transformation is conceptually difficult. As is exemplified for the dehydrochlorination of γ-HCH in Scheme 1, HCHs and some of their transformation products show conformational mobility and, therefore, exist as different conformers that can be converted into each other by ring flipping. Moreover, not all H−C−C−Cl bond arrangements are productive. Dehydrochlorination reactions leading to the elimination of HCl can only occur when H and Cl atoms align in *trans* 1,2-diaxial arrangements (exemplified by red and blue H−C−C−Cl bonds in each of the two γ-HCH conformers Cf1 and Cf2 in Scheme 1). The conformers of γ-HCH are superimposable, but the reactive positions change. This chemical phenomenon has two consequences for the biodegradation of HCHs. First, dehydrochlorination reactions may lead to different products. Second, depending on the predominant conformer, isotopically substituted atoms may or may not be located at reactive positions. It is currently unknown whether conformational mobility affects the observable isotope fractionation during enzymatic transformations of HCHs. Because enzyme-catalyzed dehydrochlorination can only occur after specific alignment of the substrate in HCH-transforming enzymes, conformational mobility could, in principle, require additional substrate release and binding steps in order to arrive at a reactive enzyme-substrate complex. Moreover,

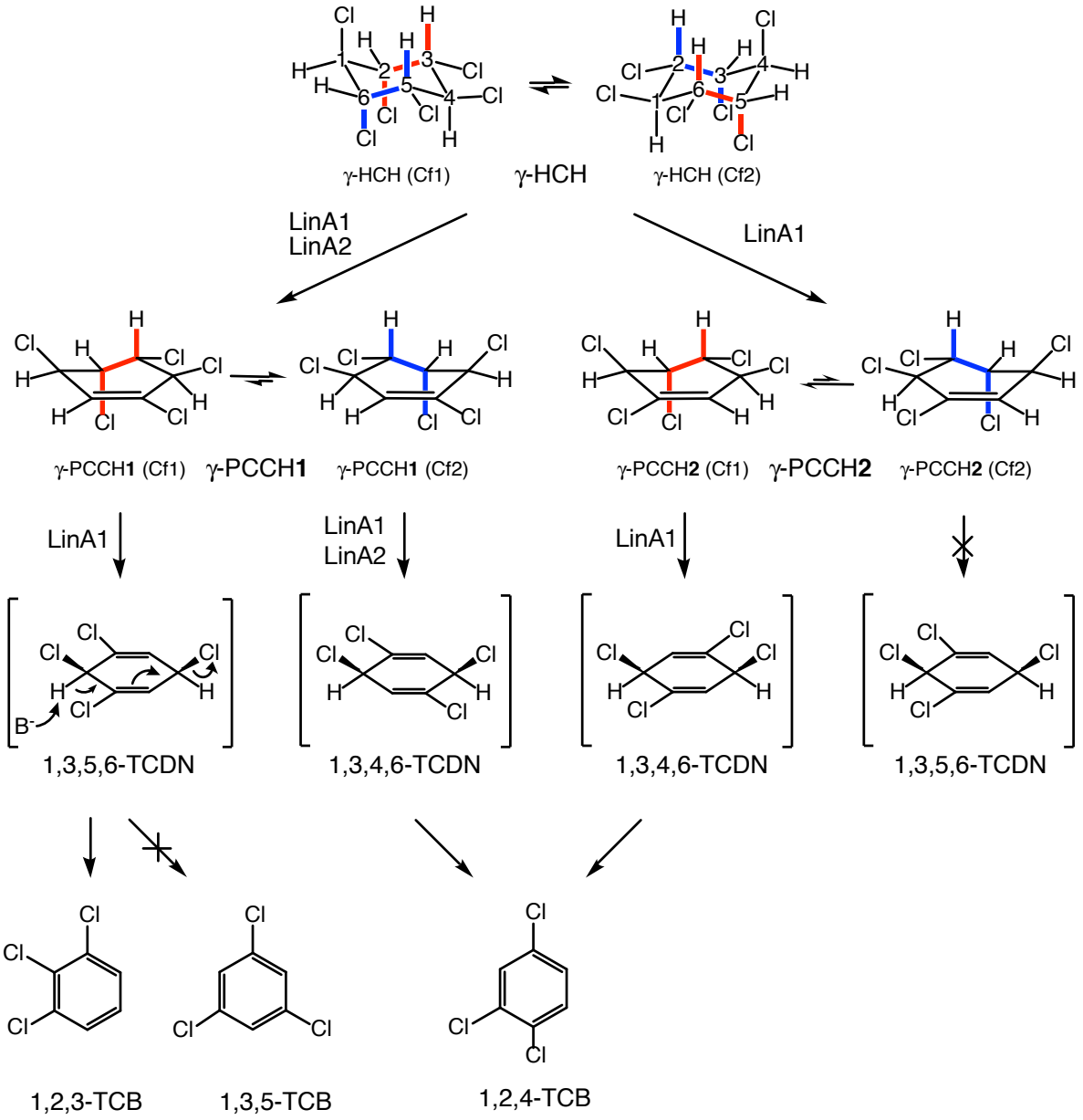

Scheme 1 Sequential dehydrochlorination of γ-hexachlorocyclohexane (γ-HCH) to γ-pentachlorocyclohexenes (γ-PCCHs), tetrachlorocyclohexadienes (TCDNs), and trichlorobenzenes (TCBs) catalyzed by the two variants of lindane dehydrochlorinases LinA1 and LinA2. Crossed arrows indicate that a reaction was not observed. The C atoms in γ-HCH are numbered for a distinction of reactive positions and isotopic substitution in the different conformers and do not represent IUPAC naming. The blue and red bonds highlight the different spatial arrangements of reactive H−C−C−Cl moieties in γ-HCH and γ-PCCH. Whereas LinA1 catalyzes the dehydrochlorination of γ-HCH at both H−C−C−Cl moieties (red and blue bonds), LinA2 only reacts with the moieties highlighted in blue in γ-HCH. Different conformers of HCH and PCCH are labelled as (Cf1) and (Cf2). γ-PCCH has two enantiomers denoted as γ-PCCH**1** (1,3(*R*),4(*S*),5(*S*),6(*R*)-γ-PCCH) and γ-PCCH**2** (1,3(*S*),4(*R*),5(*R*),6(*S*)-γ-PCCH). The stereochemical configuration of the respective TCDN stereoisomers is as follows: 1,3*(R)*,4,6*(R)*-TCDN, 1,3*(S)*,4,6*(S)*-TCDN, and 1,3(*s*),5,6(*s*)-TCDN.

different enzymes are able to catalyze the same HCH dehydrochlorination reaction and it is unknown whether the effects of conformational mobility on product formation and isotope effects are the same among these enzymes. In fact, several homologs of the lindane dehydrochlorinase LinA, the enzyme that catalyzes the first step of degradation through dehydrochlorination, have been isolated from bacteria at contaminated sites in India, Japan, and France. Whereas the enzymes share a high amino acid sequence identity (88-99 %), their catalytic efficiency and enantiospecificity are different.[1,33,34] LinA1 and LinA2 are known to discriminate among γ-HCH conformers in that LinA1 can attack the substrate at both *trans* 1,2-diaxial HCl arrangements, whereas LinA2 specifically differentiates the enantiotopical pairs of the vicinal HCl[35] and attacks only one (Scheme 1). However, the consequences of these enzyme-specificities for CSIA of HCH are still elusive.

The goal of this study was to contribute to future applications of CSIA of HCH by investigating the effects of enzyme-specificity on C and H kinetic isotope effects associated with initial steps of HCH biodegradation. To this end, (*i*) we investigated the kinetics and product distribution associated with the dehydrochlorination of γ-HCH and γ-pentachlorocyclohexene enantiomers (γ-PCCH) by LinA1 and LinA2, two variants of LinA which are known to react differently with γ-HCH and γ-PCCH (Scheme 1). (*ii*) We quantified the C and H isotope fractionation of γ-HCH associated with enzymatic dehydrochlorination and modelled enzyme and conformer specific isotope fractionation and kinetic isotope effects from experimental data. Finally, (*iii*) we compared the outcome of this evaluation with established procedures of stable isotope analysis including apparent ^{2}H and ^{13}C kinetic isotope effects (AKIE) and the correlation of C and H isotope fractionation.

Materials and Methods

Chemicals

A complete list of all chemicals, their suppliers and purities can be found in the Supporting Information Section S1. We synthesized racemic γ-PCCH from γ-HCH by alkaline dehydrochlorination according to Trantirek et al.[35] and Raina et al.[2] and the description of the synthesis and purification

procedures are shown in Section S1.3.

Purification of LinA1 and LinA2

For the expression of LinA1 and LinA2, *E. coli* BL21AI, an arabinose-inducible strain, was transformed with pDEST17 plasmid vectors encoding either a codon-optimized, synthetic and 6x His-tagged *linA1* or *linA2* as well as ampicillin resistance.[36] For enhanced folding of LinA1 and LinA2, the cells were additionally transformed with pGro7 (Takara Bio Inc.), which encodes the chaperone protein groES-groEL and chloramphenicol resistance. Information about the growing procedure and induction of enzyme expression and purification is provided in Section S2. Activity assays were performed for each purification of LinA1, and LinA2 and the results, along with SDS-Page gels are shown in Section S2.

Biotransformation Experiments

Four types of experiments were carried out with either 25 μM of γ-HCH or racemic γ-PCCH as substrate at pH 7.5 for transformation catalyzed by LinA1 or LinA2. Experiments with γ-HCH were carried out in 200 mL reactors containing 150 mL of tris-glycine buffer at initial substrate concentrations of 25 μM. Concentrations of LinA1 and LinA2 ranged from 4.1 to 4.9 and 0.51 to 0.92 μg/mL, respectively, as shown in Table S2. Experiments with γ-PCCH were carried out in 5 mL of tris-glycine buffer in 8 mL reactors containing 40 and 0.6 μg/mL of LinA1 and LinA2, respectively (Table S3). All reactors with γ-HCH were sealed with viton rubber stoppers (Maagtechnic AG) to minimize evaporative losses of substrates and products. Reactors, containing γ-PCCH as the substrate, were sealed with PTFE/silicone septa. Experiments were carried out at room temperature on an orbital shaker at 100 rpm (KS15A or SM 30A, Edmund Bühler GmbH). A total of 10 to 14 reactors were set up for each experiment. At predefined time-point, reactors were sacrificed by stopping the reaction through extraction of γ-HCH and reaction products into 25 mL of *n*-hexane. In experiments with γ-PCCH, the analytes were extracted into 2.5 mL of ethyl-acetate. *n*-Hexane contained 40 μM of 2,4-dinitrotoluene as an internal standard, which we used to account

for possible evaporation of the solvent during sample preparation. The reactors were shaken for at least 2 minutes during the liquid-liquid extraction.

Chemical and Isotopic Analyses

The concentration of γ-HCH, two γ-PCCH enantionmers, 1,2,3-TCB, 1,2,4-TCB, 1,3,5-TCB, and 2,4,-DNT we measured with a GC/MS (Trace GC Ultra with ITQ 900, Thermo Scientific) as described previously.[37] For chromatographic separation of γ-PCCH enantiomers a 30-m-chiral γ-DEX 120 column (0.25 mm i.d., 25 μm film, Supelco) was installed. The temperature program for the γ-DEX 120 column was 2 min at 70°C, 15°C/min to 110°C, 5°C/min to 200°C, 5°C/min to 220°C, and 25°C/min to 250 (held for 2 min). Helium was used as carrier gas with a constant flow of 1.5 mL/min.

We determined $^{13}C/^{12}C$ ratios in γ-HCH, γ-PCCH and TCBs and $^{2}H/^{1}H$ ratios in γ-HCH by gas chromatography isotope ratio mass spectrometry (GC/IRMS) consisting of a Trace GC equipped with a 30 m Rtx-1301 column (0.32 mm i.d., 1 μm film, 30 m length, Restek) and a Delta plus XL IRMS, Thermo Scientific. 1, 4 or 9 μL of sample or standard solution were injected in splitless mode with a splitless time of 1 min, a split flow of 30 mL/min and an injector temperature of 250°C. Note that in contrast to the analysis by GC/MS, the chromatographic resolution of our GC/IRMS system was too low to resolve enantiomers of γ-PCCH thus precluding the enantiomer-specific evaluation of stable isotope fractionation. The temperature program was 1 min at 70°C, 25°C/min to 120°C, 5°C/min to 200°C, 25°C/min to 250 (held for 10 min). $^{13}C/^{12}C$ ratios were determined with a conventional Cu/Pt reactor in the combustion interface (GC Combustion III, Thermo Scientific) at 940 °C. $^{2}H/^{1}H$ ratios were measured using an adapted method by Renpenning et al.[28]. The instrumental setup was identical with that C isotopes analysis except for analyte conversion with a custom-made, high-temperature Cr reactor operated at 1250 °C. The accuracy of isotope ratio measurement was ensured through standard bracketing procedures.[38] Standard injections included an in-house standard of γ-HCH as well as two hexachlorobenzene (HCB) specimen of known $\delta^{13}C$ from different suppliers as well as heptadecane and hexadecane reference material of known $\delta^{2}H$[39]

(Section S1.4). Isotopic calibration of $\delta^{13}C$ vs Vienna PeeDee Belemnite (VPDB) and $\delta^{2}H$ vs the Standard Mean Ocean Water (SMOV) scales, signal drift, and measurement uncertainties of triplicate injections were accounted for by using a Kragten spreadsheet[40] as proposed by Dunn et al.[41]. $\delta^{13}C$ and $\delta^{2}H$ values are reported as the average ± standard deviations of three- and five-fold measurements, respectively.

Data Analysis

Dehydrochlorination kinetics

The dehydrochlorination kinetics of γ-HCH and γ-PCCH to less chlorinated products were evaluated in a series of ordinary differential equations implemented in Copasi[42] (Section S4.1). The catalytic efficiency, k_{cat}/K_m, of the dehydrochlorination of γ-HCH and γ-PCCH catalyzed by the LinA1 and LinA2 was determined under the assumption of Michaelis-Menten kinetics based on the relationship shown in eq. 1. Due to the limited aqueous solubility of γ-HCH (<25 μM),[43] experiments had to be conducted at aqueous substrate concentrations, below enzyme saturation, that is at $S \ll K_M$ and the Michaelis-Menten kinetics then modify to

$$v = \frac{k_{cat}}{K_m} \cdot [Enz]_0 \cdot [S] = k_{obs,S} \cdot [S] \quad (1)$$

where v is the reaction rate in M/s, k_{cat} the turnover number in s^{-1}, K_m is the Michaelis constant, $[Enz]_0$ is the initial enzyme concentration, $[S]$ is the substrate concentration, and $k_{obs,S}$ is the first order dehydrochlorination rate constant obtained from kinetic modeling (Section S4.1). $[Enz]_0$ were calculated from the molar mass of the amino acid sequences (i.e., 17'145 g/mol for LinA1 and 17'341 g/mol for LinA2).[44] k_{cat}/K_m was obtained from the division of $k_{obs,S}$ by $[Enz]_0$.

Stable isotope analysis

Isotope enrichment factors, ϵ, and apparent kinetic isotope effects, AKIE, pertinent to the dehydrochlorination of γ-HCH and γ-PCCH were derived with a suite of approaches documented in

Pati et al.[38]. Information on substrate C and H isotope fractionation was obtained for γ-HCH with eq. 2.

$$\ln\left(\frac{\delta^h\mathrm{E}+1}{\delta^h\mathrm{E}_0+1}\right) = \epsilon_\mathrm{E}\cdot(\ln c/c_0) \tag{2}$$

where E stands for the elements C and H, $\delta^h\mathrm{E}_0$ and $\delta^h\mathrm{E}$ are the initial isotope signatures of the substrate and during its transformation, respectively. c/c_0 is the fraction of the remaining substrate. Apparent ^{13}C kinetic isotope effects, ^{13}C-AKIE, were calculated from ϵ_C-values following standard procedures by accounting for isotopic dilution, reactive sites, and intramolecular competition as detailed in Elsner[24] (eq. 3).

$$^{13}\text{C-AKIE} = \frac{1}{1+n/x\cdot z\cdot\epsilon_\mathrm{C}} \tag{3}$$

where n is the number of C atoms in the substrate, x is the number of these atoms at a reactive position(s) and z is the correction for intramolecular isotopic competition. As is documented in Section S4.2, the term $n/x\cdot z$ was equal to 3 regardless of the different substrate specific interactions of γ-HCH conformers (Scheme 1) with LinA1 and LinA2. Data from replicate experiments were combined using the Pitman estimator.[45] Note that eq. 3 was not applicable for the derivation of ^{2}H-AKIEs because it leads to numerical artefacts at large H isotope fractionation.[46]

Alternatively, ^{2}H-AKIEs were obtained by solving a set of ordinary differential equations for all H isotopomers (isotopic isomers[47]) containing not more than one heavy isotope as proposed previously by Wijker et al.[46] (eq. 4). ^{13}C-AKIE were derived with the same procedure for C isotopomers to illustrate the equivalence of the two approaches.

$$\frac{\mathrm{d}c_i^\mathrm{E}}{\mathrm{d}t} = \sum_i \nu_i\cdot\omega_i^\mathrm{E}\cdot k_j^\mathrm{E}\cdot c_i^\mathrm{E} \tag{4}$$

where c_i^E is the concentration of an isotopomer of element E, ν_i is the stoichiometric coefficient indicating decay or formation of an isotopomer, ω_i^E is the probability of isotopomer i to have a heavy or light isotope at the reactive position, and k_j^E is the pseudo-first-order rate constant for

reaction of an isotopomer according to the presence of the light (l) or heavy (h) isotope at the reactive position (k_l^{E} and k_h^{E}). A compilation of C and H isotopomers of γ-HCH can be found in Section S4.3 and Tables S4 and S5. Sequential dehydrochlorination reactions were modeled accordingly with eq. 4 by including isotopomers of reaction products (γ-PCCH enantiomers, TCB isomers). Ordinary differential equations were solved using the software AQUASIM[48] by fitting measured species concentrations and C or H isotope signatures to eq. 4. ^{13}C- and ^{2}H-AKIE were obtained from eq. 5.

$$^{h}\mathrm{E\text{-}AKIE} = \frac{k_l^{\mathrm{E}}}{k_h^{\mathrm{E}}} \tag{5}$$

Correlations of C and H isotope fractionation, $\Lambda^{\mathrm{H/C}}$, provided independent evidence for the ratio of the isotope enrichment factors $\epsilon_{\mathrm{H}}/\epsilon_{\mathrm{C}}$. Due to the large H isotope effects associated with the dehydrochlorination of γ-HCH, $\Lambda^{\mathrm{H/C}}$, was evaluated with the log-linear relation ship in eq 6.[46,49]

$$\Lambda^{\mathrm{H/C}} = \frac{\ln\left(\left(\delta^{2}\mathrm{H}+1\right)/\left(\delta^{2}\mathrm{H}_0+1\right)\right)}{\ln\left(\left(\delta^{13}\mathrm{C}+1\right)/\left(\delta^{13}\mathrm{C}_0+1\right)\right)} = \frac{\epsilon_{\mathrm{H}}}{\epsilon_{\mathrm{C}}} \tag{6}$$

Accounting for conformational mobility of γ-HCH

The consideration of different isotopomers of γ-HCH, containing either light or one heavy C or H isotope, with eq. 4 enabled us to take the reactions of the two different conformers of γ-HCH into account. As discussed in Section S4.3, this approach involved an explicit analysis of the reactive H−C−C−Cl moieties in both γ-HCH conformers for dehydrochlorinations by LinA1 and LinA2 separately. This explicit analysis was repeated for each of the seven C and seven H isotopomers and resulted in the quantification of isotopomer-specific ω_i^{E} and ω_i^{E} values as shown in Tables S4 and S5.

Results and Discussion

Pathways of sequential γ-HCH dehydrochlorinations catalyzed by LinA enzymes

Both variants of the hexachlorocyclohexane dehydrochlorinase, LinA1 and LinA2, catalyzed the transformation of γ-HCH to trichlorobenzenes (TCB) via γ-pentachlorocyclohexenes (γ-PCCH) and the putative tetrachlorocyclohexadienes (TCDN). The reaction pathways of γ-HCH and of the two γ-PCCH enantiomers are shown in Scheme 1 as well as in Figures S4, S5, and S6. The progress of the dehydrochlorination reactions of γ-HCH and of the two γ-PCCH enantiomers is displayed in Figure 1 and discussed below.

LinA2

LinA2 catalyzed the transformation of γ-HCH via 1,3(*R*),4(*S*),5(*S*),6(*R*)-PCCH (γ-PCCH**1**) to 1,2,4-TCB (Figure 1a). The stereochemistry of γ-PCCH**1** was assigned based on Trantirek et al.[35]. The dehydrochlorinations were completed when the concentration of 1,2,4-TCB, the final product, corresponded to the initial concentration of γ-HCH. We could rationalize the formation of the reaction products as a consequence of the preference of LinA2 for dehydrochlorination of only one of the two possible *trans* 1,2-diaxial H−C−C−Cl arrangements (highlighted in blue color in Scheme 1). Furthermore, the exclusive formation of 1,2,4-trichlorobenzene (1,2,4-TCB) implies that γ-PCCH**1** was dehydrochlorinated to the putative intermediate 1,3,4,6-tetrachlorocyclodiene (1,3,4,6-TCDN). Note that dehydrochlorination of 1,3,4,6-TCDN through *anti*-1,4-elimination was assumed to occur spontaneously and led only to 1,2,4-TCB (Scheme 1).

The progress curves shown in Figure 1 could be well described by first order kinetics (see section S4.1 and eq. S4). LinA2 catalyzed transformations of γ-HCH and γ-PCCH**1** with catalytic efficiencies k_{cat}/K_m of $(1.7 \pm 0.1) \cdot 10^4$ M^{-1} s^{-1} and $(2.9 \pm 0.1) \cdot 10^4$ M^{-1} s^{-1}, respectively (Table 1). Whereas uncertainty asscociated with repeatability of k_{cat}/K_m-values were rather small, uncertainty associated with reproducibility was more substantial (Table S2 and S3). This observation was made

for all experiments with different substrate and enzyme combinations. We attribute these variations to differences in enzyme activities of different enzyme batches as well as to uncertainties associated with determining enzyme concentrations (Sections S2 and S4.1).

In experiments with racemic mixtures of γ-PCCH**1** and γ-PCCH**2** as substrates, the rapid formation of 1,2,4-TCB was accompanied by the concomitant rapid disappearance of γ-PCCH**1**. Conversely, the slow disappearance of γ-PCCH**2** correlated well with the slow formation of 1,2,3-TCB (Figure 1b). Moreover, the added concentrations of the two substrate-product combinations (γ-PCCH**1**+1,2,4-TCB and γ-PCCH**2**+1,2,3-TCB) remained constant at 13 μM throughout the entire reaction. Therefore, we conclude that the transformation of γ-PCCH**1** and γ-PCCH**2** led to formation of 1,2,4-TCB and 1,2,3-TCB, respectively (see reaction scheme in Figure S6) in agreement with previous findings,[50] and that LinA2 showed strict preference for dehydrochlorination of only one H−C−C−Cl arrangement (marked in blue in Figure S6). The k_{cat}/K_m-value for the dehydrochlorination of γ-PCCH**1** to 1,2,4-TCB turned out to be about four times higher than that for the dehydrochlorination of γ-PCCH**2** to 1,2,3-TCB (Table 1).

LinA2 selectively transformed the thermodynamically more stable conformer Cf2 of γ-PCCH**1** to 1,3,4,6-TCDN, which spontaneously dehydrochlorinated to 1,2,4-TCB. In contrast, LinA2 preferentially dehydrochlorinated the thermodynamically less stable conformer Cf2 of γ-PCCH**2** via 1,3,5,6-TCDN as transient intermediate to 1,2,3-TCB as the final product. Note that dehydrochlorination of the less stable conformer Cf2 of γ-PCCH**2** also exhibited smaller k_{cat}/K_m-values. A detailed discussion of the logic for deducing the exact reaction scheme for LinA2 is presented in the caption of Figure S6.

LinA1

Dehydrochlorination of γ-HCH catalyzed by LinA1 led to additional transient and final reaction products (Figure 1c). LinA1 catalyzed the transformation of γ-HCH to both γ-PCCH enantiomers and congruously, we also observed the formation of both 1,2,3-TCB and 1,2,4-TCB (Figure 1c). At the end of the incubation, 1,2,4-TCB accounted for about 85% of the transformed γ-HCH whereas

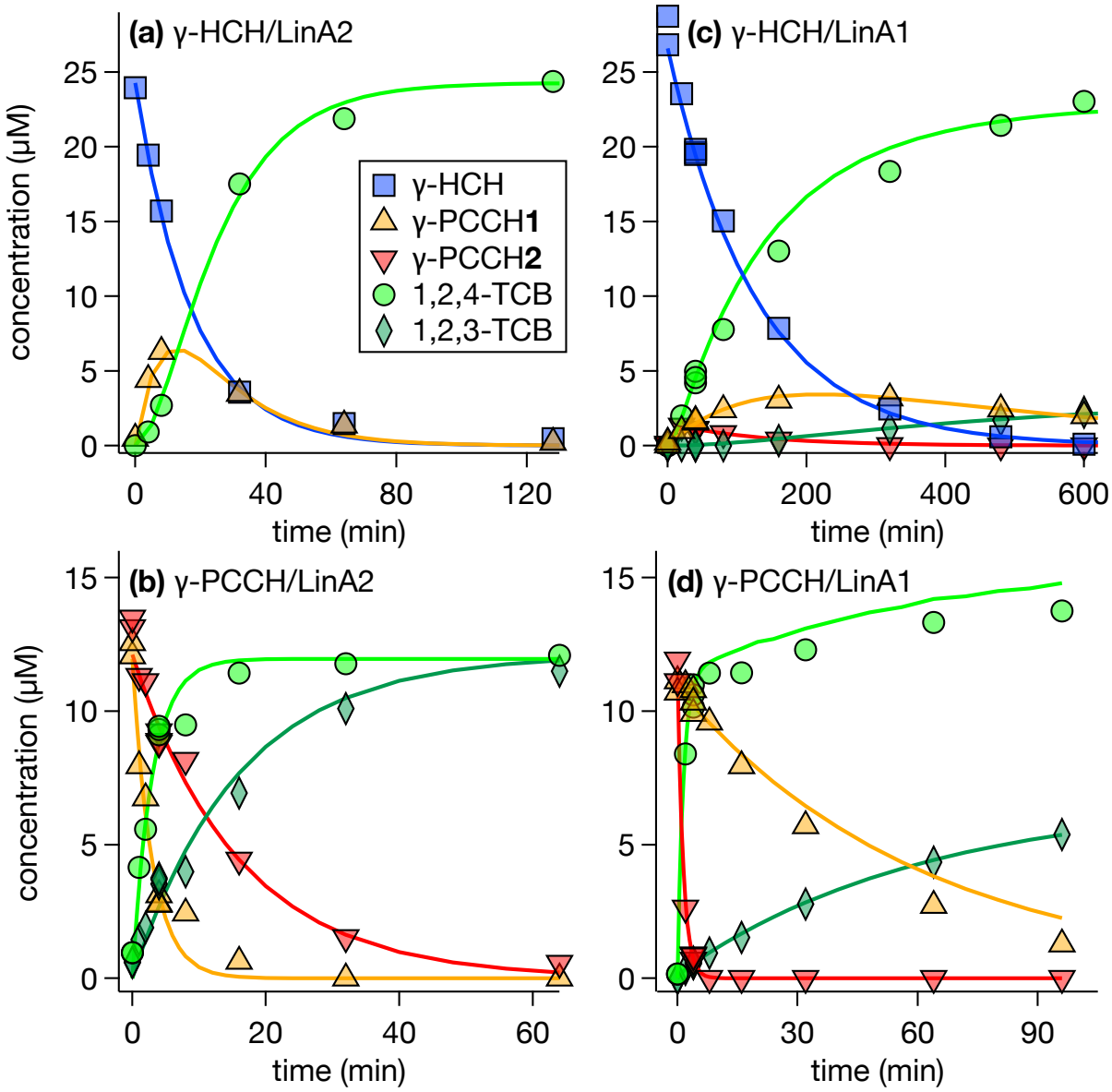

Figure 1 Kinetics of the dehydrochlorination of γ-HCH and racemic mixtures of γ-PCCH by LinA1 and LinA2. The various substrate and enzyme combinations are **(a)** γ-HCH and LinA2, **(b)** γ-PCCH and LinA2, **(c)** γ-HCH and LinA1, **(d)** γ-PCCH and LinA1. Solid lines represent best-fit lines obtained by nonlinear regression in COPASI[42] (see Section S4). Uncertainties of concentration measurements are smaller than marker sizes and not shown here.

the concentrations of 1,2,3-TCB and γ-PCCH**1** accounted for the remaining 12% to 15%. These observations imply that LinA1, in contrast to LinA2, was able to catalyze the dehydrochlorination γ-HCH at both *trans* 1,2-diaxial H−C−C−Cl arrangements (denoted in red and blue color in Scheme 1).

Best fit parameters of data fits to the reaction model (see Section S4) by nonlinear regression are summarized in Table 1. Based on the ratio of k_{cat}/K_m values, LinA1 exhibited a strong preference for transforming γ-HCH to γ-PCCH**2** as compared to transforming it to γ-PCCH**1** (Scheme 1). Moreover, in incubations with γ-HCH as the substrate, LinA1 transformed γ-PCCH**2** exclusively to 1,2,4-TCB with a rate constant that was about 100-fold larger than those for the reactions of γ-PCCH**1** either to 1,2,3-TCB or to 1,2,4-TCB. The kinetic preference for dehydrochlorination of γ-PCCH**2** to 1,2,4-TCB implies a predominant formation of the putative 1,3,4,6-TCDN from γ-PCCH**2** conformer Cf1 (Scheme 1). In contrast, dehydrochlorination of γ-PCCH**1** involved both conformers, Cf1 and Cf2, and both putative TCDN isomers.

Experiments with LinA1 and racemic mixtures of γ-PCCH**1** and γ-PCCH**2** confirmed the enantiomer and conformer specificity of γ-HCH dehydrochlorination by LinA1 (Figures 1d and S5). However, in such incubations the data fits gave indication that γ-PCCH**2** was also transformed to 1,2,3-TCB, most likely by dehydrochlorination of conformer Cf2. k_{cat}/K_m values for dehydrochlorination γ-PCCH**2** to 1,2,4-TCB (Table 1) again exceeded those for γ-PCCH**1** either to 1,2,3-TCB or to 1,2,4-TCB by two orders of magnitude. The preferential formation of 1,2,4-TCB was also consistent with the fact that γ-PCCH**1** conformer Cf2 and γ-PCCH**2** conformer Cf1 were thermodynamically more stable (Section S3) and thus more available to react with LinA1.

The comparison of the dehydrochlorination kinetics of the two LinA variants illustrates that LinA1 predominantly catalyzed the transformation γ-HCH to γ-PCCH**2** and 1,2,4-TCB whereas LinA2 exclusively catalyzed the transformation of γ-HCH to γ-PCCH**1** and 1,2,4-TCB. Note that no 1,3,5-TCB was detected in any of our experiments even though this TCB isomer could have been formed theoretically from both γ-PCCH enantiomers.

Table 1 Catalytic efficiency k_{cat}/K_m, of LinA1 and LinA2 for different reactions, C and H isotopic enrichment factors (ϵ_C, ϵ_H), $\Lambda^{H/C}$ values, H- and C- apparent kinetic isotope effects.[a]

parameter	units	reaction	LinA1		LinA2	
			γ-HCH	γ-PCCH	γ-HCH	γ-PCCH
k_{cat}/K_m	($M^{-1}s^{-1}$)	γ-HCH → γ-PCCH**1**	$(1.0 \pm 0.1)\cdot10^2$	-[b]	$(1.7 \pm 0.1)\cdot10^4$	-
		γ-HCH → γ-PCCH**2**	$(3.6 \pm 0.1)\cdot10^2$	-	-	-
		γ-PCCH**1** → 1,2,4-TCB	$(6.5 \pm 0.1)\cdot10^1$	$(9.5 \pm 0.1)\cdot10^1$	$(2.9 \pm 0.1)\cdot10^4$	$(2.7 \pm 0.1)\cdot10^2$
		γ-PCCH**1** → 1,2,3-TCB	$(7.6 \pm 0.1)\cdot10^1$	$(1.5 \pm 0.1)\cdot10^2$	-	-
		γ-PCCH**2** → 1,2,4-TCB	$(6.7 \pm 0.1)\cdot10^3$	$(1.0 \pm 0.1)\cdot10^4$	-	-
		γ-PCCH**2** → 1,2,3-TCB	-	$(1.4 \pm 0.1)\cdot10^2$	-	$(6.7 \pm 0.2)\cdot10^1$
ϵ_C [c]	(‰)	γ-HCH → γ-PCCH	–8.1 ± 0.3	-	–8.3 ± 0.2	-
ϵ_H [c]	(‰)	γ-HCH → γ-PCCH	–122 ± 6	-	–160 ± 6	-
$\Lambda^{H/C}$ [d]	(-)	γ-HCH → γ-PCCH	11.5 ± 0.8	-	16.4 ± 0.9	-
^{13}C-AKIE [e]	(-)	γ-HCH → γ-PCCH	1.024 ± 0.001	-	1.025 ± 0.001	-
^{13}C-AKIE [f]	(-)	γ-HCH → γ-PCCH	1.023 ± 0.0005	-	1.027 ± 0.0005	-
^{2}H-AKIE [f]	(-)	γ-HCH → γ-PCCH	2.4 ± 0.1	-	2.6 ± 0.1	-

[a] Uncertainties represent 95% confidence intervals [b] - = not detected; [c] eq. 2 [d] eq. 6 [e] calculated from ϵ_C-values with eq. 3
[f] derived from isotopomer-specific model with eq. 4

Isotope fractionation associated with the LinA2-catalyzed dehydrochlorination of γ-HCH

Carbon Isotope fractionation

The dehydrochlorination of γ-HCH by LinA2 to γ-PCCH**1** was accompanied by considerable C isotope fractionation (Figure 2a) and the corresponding C isotope enrichment factor, ϵ_C, obtained from eq. 2, was -8.3 ± 0.2‰ (Table 1). A series of independent observations supported the large ϵ_C-value. First, the difference between the initial $\delta^{13}C$ of γ-HCH and the $\delta^{13}C$ of γ-PCCH**1** at low substrate conversion, which can be used here to approximate ϵ_C, also amounted to -7.7 ± 0.3‰. Second, the ϵ_C value for transformation of γ-HCH to γ-PCCH**1** derived with an isotopomer-specific model (eq. 4) was -8.7 ± 0.1‰ (Table S6). The minor differences between the results of the different calculation methods confirm the substantial C isotope fractionation and agree with previous observations made for systematic comparison of alternative data evaluation procedures.[38] The $\delta^{13}C$ of the accumulating product 1,2,4-TCB of -25.8 ± 0.1‰ matched the initial $\delta^{13}C$ of γ-HCH (-25.9 ± 0.1‰) indicating a complete isotopic mass balance. We also determined an ϵ_C of -6.9 ± 0.7‰ (Table S6) for the sequential dehydrochlorinations of γ-PCCH**1** conformer Cf1 to 1,3,4,6-tetrachlorocyclohexadiene (1,3,4,6-TCDN) and its *anti*-1,4-elimination to 1,2,4-TCB (Scheme 1) in the same data evaluation procedure. While a mechanistic interpretation of the two consecutive reactions is not possible, this data confirms the large C isotope fractionation associated with enzyme-catalyzed dehydrochlorination processes.

The observed C isotope fractionation originated from the dehydrochlorination of the H$-C_5-C_6-$Cl and H$-C_2-C_3-$Cl moieties of γ-HCH conformers Cf1 and Cf2, respectively, which are highlighted as blue bonds in Scheme 1. As was illustrated above in the analysis of the reaction progress of γ-HCH dehydrochlorination by LinA2 (Figure 1a), different equatorial and axial relationships of the H and Cl atoms in γ-HCH conformer Cf1, H$-C_3-C_2-$Cl, and conformer Cf2, H$-C_6-C_5-$Cl, (red bonds in Scheme 1) were not reactive with LinA2. This selectivity of LinA2 had consequences for the assignment of reactive positions in γ-HCH and thus for the derivation of apparent kinetic

isotope effects (AKIE). γ-HCH exhibited four C atoms in two reactive H−C−C−Cl moieties from which dehydrochlorinations can occur. However, because conformers Cf1 and Cf2 could interconvert through ring flipping and because both conformers were of equal thermodynamic stability and abundance (see Sections S3 and S4.2), γ-HCH would, on average, only feature two reactive C atoms in one H−C−C−Cl moiety that could undergo dehydrochlorination by LinA2. Based on this mechanistic interpretation, we derived an apparent ^{13}C kinetic isotope effect, ^{13}C-AKIE, of 1.025 ± 0.001 with eq. 3 (Table 1). We obtained a slightly higher ^{13}C-AKIE of 1.027 ± 0.0005 using a set of ordinary differential equations (eq. 4, Table S6). This procedure accounts explicitly for ^{12}C and ^{13}C isotopomers and leads to smaller uncertainty estimates because the error in the ϵ_C-value no longer scales with the correction for isotopic dilution.[38,46] Furthermore, the good agreement of ^{13}C-AKIEs confirmed our assumptions on the reactivity of different γ-HCH conformers outlined in detail in Sections S4.2 and S4.3.

Hydrogen Isotope fractionation

The H isotope fractionation associated with the same dehydrochlorination experiment of γ-HCH by LinA2 is shown in Figure 1b. We observed substantial H isotope fractionation corresponding to an ϵ_H-value of $-160 \pm 6‰$ (Table 1). The interpretation of H isotope fractionation in terms of ^{2}H-AKIEs for the dehydrochlorination reaction followed the reasoning established for ^{13}C-AKIE, and we assumed that one of six H atoms of γ-HCH was in a reactive H−C−C−Cl moiety. However, as reported previously,[46,49,51] quantification of ^{2}H-AKIEs from large H isotope fractionation with eq. 3 does not lead to chemically meaningful results. Here, use of eq. 3 would have resulted in a ^{2}H-AKIE of 25 and thus strongly overestimated the magnitude of H isotope fractionation in a dehydrohalogenation (i.e., elimination) reaction.[52–55] By applying the isotopomer-specific model for the interpretation of H isotope fractionation, we arrived at a ^{2}H-AKIE of 2.6 ± 0.1 (Table 1), which is discussed regarding dehydrochlorination mechanisms in detail below.

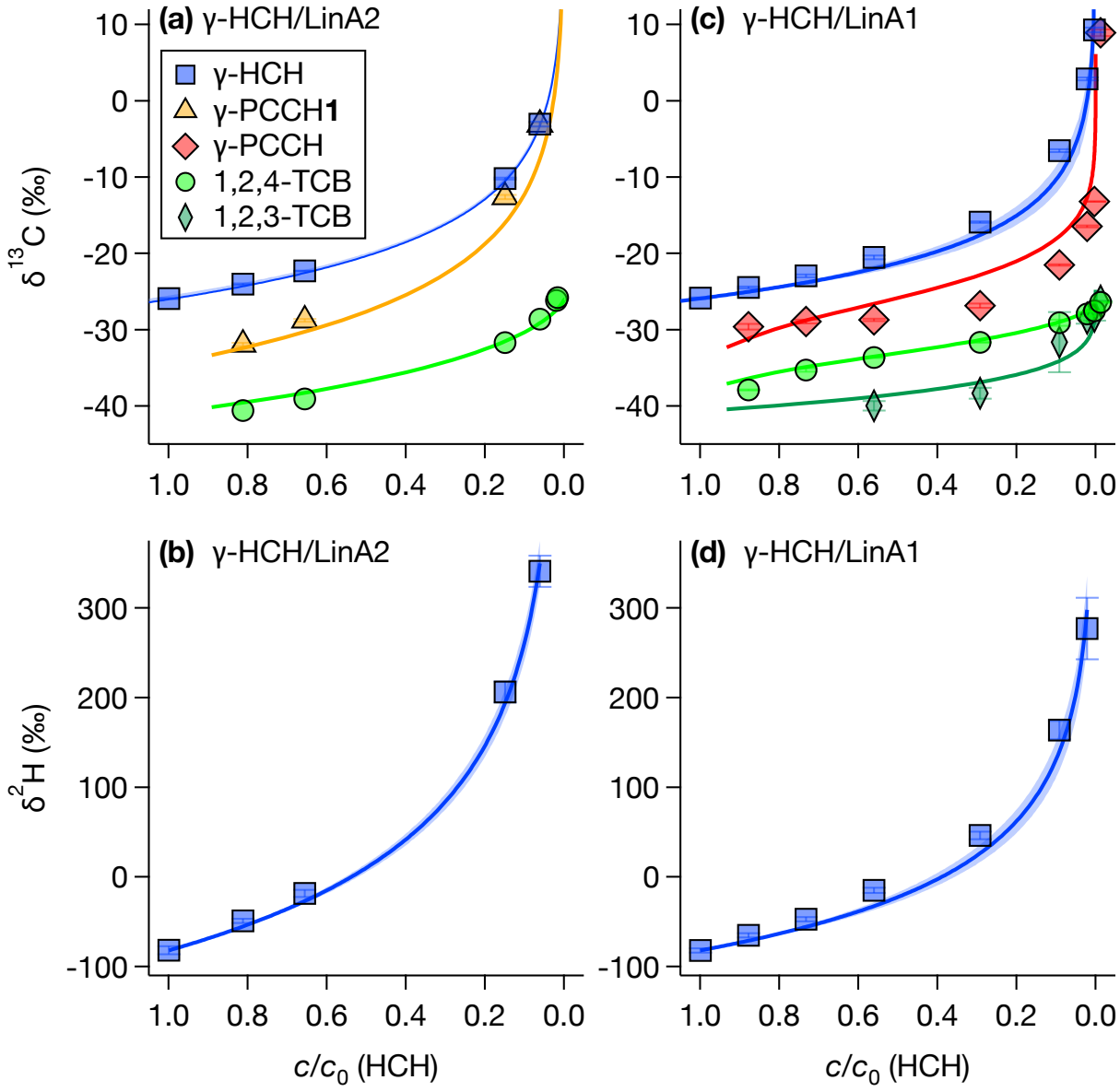

Figure 2 C and H isotope fractionation associated with the dehydrochlorination of γ-HCH by LinA2 and LinA1. Panels **(a)** and **(b)** show δ^{13}C and δ^{2}H trends for experiments with LinA2, respectively, whereas panels **(c)** and **(d)** illustrate the same data obtained with LinA1. The solid lines reflect the isotope fractionation behaviour calculated with eq. 4. Shaded areas indicate 95% confidence intervals for model fits for γ-HCH.

C and H isotope fractionation associated with the LinA1-catalyzed dehydrochlorination of γ-HCH

The C and H isotope fractionation associated with the dehydrochlorination of γ-HCH catalyzed by LinA1 is shown in Figures 2c/d. The C isotope fractionation was large, and the ϵ_C of $-8.1 \pm 0.3‰$ was identical within uncertainty to the dehydrochlorination of γ-HCH catalyzed by LinA2 (Table 1). The H isotope fractionation was again large, but the ϵ_H-value $-122 \pm 6‰$ was considerably smaller than for dehydrochlorination catalyzed by LinA2. δ^{13}C values for γ-PCCH and two TCB isomers confirmed the above observations that large C isotope fractionation accompanied the sequential dehydrochlorinations. At the end of the experiment with LinA1, the averaged δ^{13}C of the remaining 1,2,4-TCB, 1,2,3-TCB and traces of γ-PCCH was $-26.0 \pm 0.1‰$ and thus identical to the initial C isotope signature of γ-HCH ($-25.9 \pm 0.1‰$). The complete isotopic mass balance confirmed that all intermediates and products were accounted for in our analyses.

The lack of chromatographic resolution impeded a quantification of ϵ_C for the individual reactions of γ-HCH $\rightarrow$ γ-PCCH**1** and γ-HCH $\rightarrow$ γ-PCCH**2**. Derivation of an ϵ_C of $-8.4 \pm 0.7‰$ (Table S6) with eq. 4 for the sequence of parallel dehydrochlorination reactions shown in Scheme 1 with an average δ^{13}C for both γ-PCCH enantiomers confirmed the large C isotope fractionation caused by LinA1-catalyzed dehydrochlorinations. The distinct trendlines for δ^{13}C of 1,2,3-TCB and 1,2,4-TCB in Figure 2c implied different magnitudes of C isotope fractionation for the reactions to the two γ-PCCH enantiomers, as well as from the two γ-PCCH enantiomers to TCB isomers. However, due to the absence of δ^{13}C values for each γ-PCCH enantiomer, we were unable to assign unequivocal ϵ_C-values to these reactions. Therefore, the fit results in Table S6 presumably overemphasize the C isotope fractionation associated with the reaction γ-PCCH $\rightarrow$ 1,2,3-TCB.

LinA1 catalyzed the dehydrochlorination of γ-HCH at two H$-$C$-$C$-$Cl moieties in each conformer and we discuss the consequences of conformational mobility for C isotope fractionation here. Conformational mobility altered the identity of the C atoms from which H^+ and Cl^- are eliminated, for example H$-C_5-C_6-$Cl in conformer Cf1 vs H$-C_6-C_5-$Cl in conformer Cf2 (Scheme 1). Because isotope fractionation of dehydrochlorinations arose from a concerted reaction at both

C atoms and both γ-HCH conformers were of equal abundance, conformational mobility did not affect the number of reactive atoms. The ^{13}C-AKIE determined with eq. 4 based on this mechanistic assumptions was 1.023 ± 0.0005 (Table 1). These values reflect the weighted average of dehydrochlorinations at two distinct *trans*-1,2-diaxial H−C−C−Cl moieties. In fact, catalytic efficiencies of LinA1 for formation of γ-PCCH**2** were 3.6 times higher than for formation of γ-PCCH**1** (see k_{cat}/K_m-values in Table 1) suggesting that ^{13}C-AKIEs were determined primarily (i.e., to 78%) by the reaction at the H−C_3−C_2−Cl (Cf1) and H−C_6−C_5−Cl (Cf2) moieties highlighted in red in Scheme 1. Assuming that isotope effects from dehydrochlorination at the H−C_5−C_6−Cl (Cf1) and H−C_2−C_3−Cl (Cf2) moieties to γ-PCCH1 highlighted in blue would correspond to those determined from γ-HCH transformation by LinA2, the ^{13}C- and ^{2}H-AKIE associated with reactions at the H−C_3−C_2−Cl (Cf1) and H−C_6−C_5−Cl (Cf2) moieties to γ-PCCH2 highlighted in red would amount to 1.022 ± 0.001 (eqs. S6 - S8). The differences between ^{13}C-AKIE values derived tentatively for the two distinct *trans*-1,2-diaxial H−C−C−Cl moieties were, however, rather small and cannot explain the difference of δ^{13}C in 1,2,4- and 1,2,3-TCB. Our data for C isotope fractionation suggests that those variabilities were within the uncertainty of parameter values derived with different approaches (i.e., eq. 3 vs eq. 4). We conclude that there was no evidence to assume that the ^{13}C-AKIEs for dehydrochlorination of γ-HCH by LinA1 at the two *trans*-1,2-diaxial H−C−C−Cl arrangements would be different. By applying the isotopomer-specific model for the interpretation of H isotope fractionation, we arrived at a ^{2}H-AKIE of 2.4 ± 0.1 (Table 1).

Enzyme specificity of C and H isotope fractionation for dehydrochlorination reactions of γ-HCH

The correlation of C and H isotope fractionation for γ-HCH dehydrochlorination by LinA1 and LinA2 based on eq 6 is shown in Figure 3. The correlation slopes, $\Lambda^{H/C}$, consistently reflect the trends of ϵ_H/ϵ_C-values (Table 1) with larger H isotope fractionation for γ-HCH dehydrochlorination by LinA2 compared to the reaction by LinA1 and thus illustrate some enzyme specificity. The apparent differences in H isotope fractionation imply subtle differences in the mechanisms of

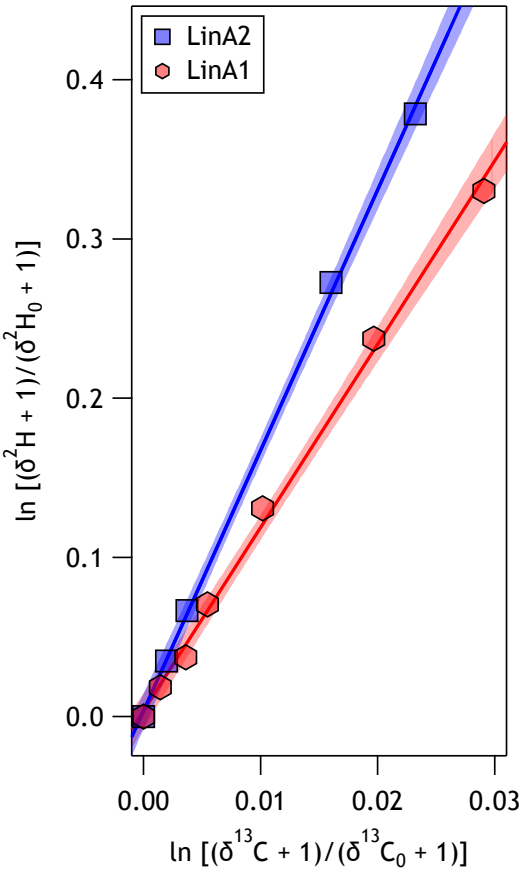

Figure 3 Correlation of H and C isotope fractionation during the dehydrochlorinatin of γ-HCH by LinA2 (blue) and LinA1 (red). Solid lines and shaded areas indicate correlation slopes $\Lambda^{H/C}$ and 95% confidence interval (LinA2: 16.4 ± 0.9; LinA1: 11.5 ± 0.8, Table 1).

dehydrochlorination. In fact, differences in ^{2}H-AKIEs in elimination reactions have been interpreted as differences in transition state structure where one distinguishes the timing of proton abstraction and leaving group departure.[52–56] Such interpretations have been applied in theoretical studies with LinA to assess concerted vs step-wise dehydrochlorination mechanisms for different HCH isomers (γ- and β-HCH).[32,57,58] Evidence from our data indicates that such differences may also arise for the same HCH-isomer when different LinA variants catalyze dehydrochlorination. Previous works suggested that the protonation state of the His73 residue is responsible for H abstraction from HCH and determines the extent of C–H bond cleavage in the transition state.[57,58] We hypothesize that this phenomenon could also have modulated the ^{2}H-AKIE of the dehydrochlorination by LinA1 and LinA2. However, an elucidation of transition state structures was beyond the scope of our work

and we noted that the theoretically derived isotope effects for γ-HCH dehydrochlorination (smaller ^{13}C AKIE from 1.0125 to 1.0193 and larger ^{2}H-AKIE between 4.1 and 5.1[32]) are quite different from the experimental evidence presented here.

Environmental Implications

Our work illustrates that the C and H isotope fractionation associated with dehydrochlorination reactions of γ-HCH is substantial, independent of HCH conformational mobility, and potentially indicative of processes initiating biodegradation of γ-HCH under aerobic conditions. However, isotopic analysis of HCH transformations in whole cell systems of *Sphingobium indicum* B90A and *Sphingobium japonicum* UT26 revealed much smaller C isotope fractionation with ϵ_C-values of $-1.5 \pm 0.1‰$ and $-1.7 \pm 0.2‰$.[15] Recent works on the magnitude of contaminant isotope fractionation during biotransformation suggested that contaminant transport across the outer membrane of gram-negative bacteria may limit the rates of substrate uptake and thus masks the observable isotope fractionation.[59,60] Such an interpretation could also apply for gram-negative, HCH-degrading bacteria.[1] The differences between ϵ_C-values for dehydrochlorination of γ-HCH obtained in LinA assays with pure enzymes and in whole cell experiments,[12,16] however, are considerably larger than effects associated with the masking of substrate isotope fractionation by uptake limitations. In fact, microorganisms such as *Sphingobium japonicum* UT26, carry glycosphingolipids in their outer membranes and are thought to utilize transporter systems to control substrate uptake as well as membrane physiology during γ-HCH degradation.[61] The consequences of active substrate uptake for HCH transformation and isotope fractionation are unfortunately unknown. Further work is warranted to elucidate the effect of HCH uptake and transport on the observable HCH isotope fractionation and the utility of CSIA to assesses biodegradation at contaminated sites.

Acknowledgement

This work was supported by the SNSF (grant no. 200021-153534). We thank Thomas Fleischmann for analytical support and Daniel Rentsch for NMR analysis.

Supporting Information Available

List of chemicals used, synthesis procedure for γ-PCCH, conformational analysis of γ-HCH, and γ-PCCH, protein purification and data evaluation procedures, reaction schemes for sequential dehydrochlorination of γ-PCCH enantiomers by LinA1 and LinA2. This material is available free of charge via the Internet at `http://pubs.acs.org/`.

References

(1) Lal, R.; Pandey, G.; Sharma, P.; Kumari, K.; Malhotra, S.; Pandey, R.; Raina, V.; Kohler, H.-P. E.; Holliger, C.; Jackson, C.; Oakeshott, J. G. Biochemistry of microbial degradation of hexachlorocyclohexane and prospects for bioremediation. *Microbiol. Mol. Biol. R.* **2010**, *74*, 58–80.

(2) Raina, V.; Rentsch, D.; Geiger, T.; Sharma, P.; Buser, H. R.; Holliger, C.; Lal, R.; Kohler, H.-P. E. New metabolites in the degradation of α- and γ-hexachlorocyclohexane (HCH): pentachlorocyclohexenes are hydroxylated to cyclohexenols and cyclohexenediols by the haloalkane dehalogenase LinB from *Sphingobium indicum* B90A. *J. Agric. Food Chem.* **2008**, *56*, 6594–6603.

(3) Vijgen, J.; Abhilash, P.; Li, Y.; Lal, R.; Forter, M.; Torres, J.; Singh, N.; Yunus, M.; Tian, C.; Schaeffer, A.; Weber, R. Hexachlorocyclohexane (HCH) as new Stockholm Convention POPs - global perspective on the management of lindane and its waste isomers. *Environ. Sci. Pollut. Res.* **2011**, *18*, 152–162.

(4) Vijgen, J.; Aliyeva, G.; Weber, R. The forum of the International HCH and Pesticides As-

sociation - A platform for international cooperation. *Environ. Sci. Pollut. Res.* **2012**, *20*, 2081–2086.

(5) Stockholm Convention, http://chm.pops.int/Home/tabid/2121/Default.aspx, Accessed: 2017-03-24.

(6) Vijgen, J. *The legacy of lindane HCH isomer production. A global overview of residue management, formulation and disposal*; International HCH & Pesticides Association (IHPA), http://www.ihpa.info/docs/library/reports/Lindane%20Main%20Report%20DEF20JAN06.pdf, 2006.

(7) International HCH & Pesticides Associsation (IHPA), http://www.ihpa.info/, Accessed: 2017-03-24.

(8) Jit, S. et al. Evaluation of hexachlorocyclohexane contamination from the last lindane production plant operating in India. *Environ. Sci. Pollut. Res.* **2011**, *18*, 586–597.

(9) Imai, R.; Nagata, Y.; Senoo, K.; Wada, H.; Fukuda, M.; Takagi, M.; Yano, K. Dehydrochlorination of γ-hexachlorocyclohexane (γ-BHC) by γ-BHC-assimilating *Pseudomonas paucimobilis*. *Agricultural and biological chemistry* **1989**, *53*, 2015–2017.

(10) Nagata, Y.; Miyauchi, K.; Takagi, M. Complete analysis of genes and enzymes for γ-hexachlorocyclohexane degradation in *Spingomonas paucimobilis* UT26. *J. Ind. Microbiol. Biot.* **1999**, *23*, 380–390.

(11) Ivdra, N.; Fischer, A.; Herrero-Martín, S.; Giunta, T.; Bonifacie, M.; Richnow, H.-H. Carbon, hydrogen and chlorine stable isotope fingerprinting for forensic investigation on Hexachlorocyclohexanes. *Environ. Sci. Technol.* **2017**, *51*, 446–454.

(12) Liu, Y.; Bashir, S.; Stollberg, R.; Trabitzsch, R.; Weiß, H.; Paschke, H.; Nijenhuis, I.; Richnow, H.-H. Compound specific and enantioselective stable isotope analysis as tools

to monitor transformation of hexachlorocyclohexane (HCH) in a complex aquifer system. *Environ. Sci. Technol.* **2017**, *51*, 8909–8916.

(13) Chartrand, M.; Passeport, E.; Rose, C.; Lacrampe-Couloume, G.; Bidleman, T. F.; Jantunen, L. M.; Sherwood Lollar, B. Compound specific isotope analysis of hexachlorocyclohexane isomers: a method for source fingerprinting and field investigation of in situ biodegradation. *Rapid Commun. Mass Spectrom.* **2015**, *29*, 505–514.

(14) Zhang, N.; Bashir, S.; Qin, J.; Schindelka, J.; Fischer, A.; Nijenhuis, I.; Herrmann, H.; Wick, L. Y.; Richnow, H. H. Compound-specific stable isotope analysis (CSIA) to characterize transformation mechanisms of α-hexachlorocyclohexane. *J. Hazard. Mater.* **2014**, *280*, 750–757.

(15) Bashir, S.; Fischer, A.; Nijenhuis, I.; Richnow, H.-H. Enantioselective carbon stable isotope fractionation of hexachlorocyclohexane during aerobic biodegradation by Sphingobium spp. *Environ. Sci. Technol.* **2013**, *47*, 11432–11439.

(16) Bashir, S.; Hitzfeld, K. L.; Gehre, M.; Richnow, H. H.; Fischer, A. Evaluating degradation of hexachlorcyclohexane (HCH) isomers within a contaminated aquifer using compound-specific stable carbon isotope analysis (CSIA). *Water Res.* **2015**, *71*, 187–196.

(17) Badea, S.-L.; Vogt, C.; Weber, S.; Danet, A.-F.; Richnow, H.-H. Stable isotope fractionation of γ-hexachlorocyclohexane (lindane) during reductive dechlorination by two strains of sulfate-reducing bacteria. *Environ. Sci. Technol.* **2009**, *43*, 3155–3161.

(18) Lian, S.; Nikolausz, M.; Nijenhuis, I.; Francisco Leite, A.; Richnow, H.-H. Biotransformation and inhibition effects of hexachlorocyclohexanes during biogas production from contaminated biomass characterized by isotope fractionation concepts. *Bioresour. Technol.* **2018**, *250*, 683–690.

(19) Elsner, M.; Zwank, L.; Hunkeler, D.; Schwarzenbach, R. P. A new concept linking observable

stable isotope fractionation to transformation pathways of organic pollutants. *Environ. Sci. Technol.* **2005**, *39*, 6896–6916.

(20) Aelion, C. M.; Höhener, P.; Hunkeler, D.; Aravena, R. *Environmental isotopes in biodegradation and bioremediation*; CRC Press, 2010.

(21) Hofstetter, T. B.; Schwarzenbach, R. P.; Bernasconi, S. M. Assessing transformation processes of organic compounds using stable isotope fractionation. *Environ. Sci. Technol.* **2008**, *42*, 7737–7743.

(22) Qiu, S.; Eckert, D.; Cirpka, O. A.; Huenniger, M.; Knappett, P.; Maloszewski, P.; Meckenstock, R. U.; Griebler, C.; Elsner, M. Direct experimental evidence of non-first order degradation kinetics and sorption-induced isotopic fractionation in a mesoscale aquifer: $^{13}C/^{12}C$ analysis of a transient toluene pulse. *Environ. Sci. Technol.* **2013**, *47*, 6892–6899.

(23) Carbon, Hydrogen, and Nitrogen Isotope Fractionation During Light-Induced Transformations of Atrazine. *Environ. Sci. Technol.* **2008**, *42*, 7751–7756.

(24) Elsner, M. Stable isotope fractionation to investigate natural transformation mechanisms of organic contaminants: principles, prospects and limitations. *J. Environ. Monit.* **2010**, *12*, 2005–2031.

(25) Pati, S. G.; Shin, K.; Skarpeli-Liati, M.; Bolotin, J.; Eustis, S. N.; Spain, J. C.; Hofstetter, T. B. Carbon and nitrogen isotope effects associated with the dioxygenation of aniline and diphenylamine. *Environ. Sci. Technol.* **2012**, *46*, 11844–11853.

(26) Cretnik, S.; Thoreson, K. A.; Bernstein, A.; Ebert, K.; Buchner, D.; Laskov, C.; Haderlein, S.; Shouakar-Stash, O.; Kliegman, S.; McNeill, K.; Elsner, M. Reductive dechlorination of TCE by chemical model systems in comparison to dehalogenating bacteria: Insights from dual element isotope analysis (13C/12C, 37Cl/35Cl). *Environ. Sci. Technol.* **2013**, *47*, 6855–6863.

(27) Nijenhuis, I.; Stollberg, R.; Lechner, U. Anaerobic microbial dehalogenation and its key players in the contaminated Bitterfeld-Wolfen megasite. *FEMS Microbiol. Ecol.* **2018**, *94*, fiy012.

(28) Renpenning, J.; Kummel, S.; Hitzfeld, K. L.; Schimmelmann, A.; Gehre, M. Compound-specific hydrogen isotope analysis of heteroatom-bearing compounds via gas chromatography–chromium-based high-temperature conversion (Cr/HTC)–isotope ratio mass spectrometry. *Anal. Chem.* **2015**, *87*, 9443–9450.

(29) Renpenning, J.; Horst, A.; Schmidt, M.; Gehre, M. Online isotope analysis of $^{37}Cl/^{35}Cl$ universally applied for semi-volatile organic compounds using GC-MC-ICPMS. *J. Anal. At. Spectrom.* **2018**, *33*, 314–321.

(30) Gehre, M.; Renpenning, J.; Geilmann, H.; Qi, H.; Coplen, T. B.; Kümmel, S.; Ivdra, N.; Brand, W. A.; Schimmelmann, A. Optimization of on-line hydrogen stable isotope ratio measurements of halogen- and sulfur-bearing organic compounds using elemental analyzer–chromium/high-temperature conversion isotope ratio mass spectrometry (EA-Cr/HTC-IRMS). *Rapid Commun. Mass Spectrom.* **2017**, *31*, 475–484.

(31) Renpenning, J.; Schimmelmann, A.; Gehre, M. Compound-specific hydrogen isotope analysis of fluorine-, chlorine-, bromine- and iodine-bearing organics using gas chromatography-chromium-based high-temperature conversion (Cr/HTC) isotope ratio mass spectrometry. *Rapid Commun. Mass Spectrom.* **2017**, *31*, 1095–1102.

(32) Manna, R. N.; Dybala-Defratyka, A. Insights into the elimination mechanisms employed for the degradation of different hexachlorocyclohexane isomers using kinetic isotope effects and docking studies. *J. Phys. Org. Chem.* **2013**, *26*, 797–804.

(33) Nagata, Y.; Endo, R.; Ito, M.; Ohtsubo, Y.; Tsuda, M. Aerobic degradation of lindane (γ-hexachlorocyclohexane) in bacteria and its biochemical and molecular basis. *Appl. Microbiol. Biotechnol.* **2007**, *76*, 741.

(34) Pal, R.; Bala, S.; Dadhwal, M.; Kumar, M.; Dhingra, G.; Prakash, O.; Prabagaran, S. R.; Shivaji, S.; Cullum, J.; Holliger, C.; Lal, R. Hexachlorocyclohexane-degrading bacterial strains *Sphingomonas paucimobilis* B90A, UT26 and Sp+, having similar *lin* genes, represent three distinct species, *Sphingobium indicum* sp. nov., *Sphingobium japonicum* sp. nov. and *Sphingobium francense* sp. nov., and reclassification of [*Sphingomonas*] *chungbukensis* as *Sphingobium chungbukense* comb. nov. *Int. J. Syst. Evol. Micr.* **2005**, *55*, 1965–1972.

(35) Trantirek, L.; Hynkova, K.; Nagata, Y.; Murzin, A.; Ansorgova, A.; Sklenar, V.; Damborsky, J. Reaction mechanism and stereochemistry of γ-hexachlorocyclohexane dehydrochlorinase LinA. *J. Biol. Chem.* **2001**, *276*, 7734–7740.

(36) Bala, K.; Geueke, B.; Miska, M. E.; Rentsch, D.; Poiger, T.; Dadhwal, M.; Lal, R.; Holliger, C.; Kohler, H.-P. E. Enzymatic conversion of ϵ-hexachlorocyclohexane and a heptachlorocyclohexane isomer, two neglected components of technical hexachlorocyclohexane. *Environ. Sci. Technol.* **2012**, *46*, 4051–4058.

(37) Geueke, B.; Garg, N.; Ghosh, S.; Fleischmann, T.; Holliger, C.; Lal, R.; Kohler, H.-P. E. Metabolomics of hexachlorocyclohexane (HCH) transformation: ratio of LinA to LinB determines metabolic fate of HCH isomers. *Environ. Microbiol.* **2013**, *15*, 1040–1049.

(38) Pati, S. G.; Kohler, H.-P. E.; Hofstetter, T. B. Characterization of substrate, cosubstrate, and product isotope effects associated with enzymatic oxygenations of organic compounds based on compound-specific isotope analysis. In *Measurement and Analysis of Kinetic Isotope Effects*; Harris, M. E., Anderson, V. E., Eds.; Methods in Enzymology; Academic Press, 2017; Vol. 596; pp 291–329.

(39) Schimmelmann, A. et al. Organic Reference Materials for Hydrogen, Carbon, and Nitrogen Stable Isotope-Ratio Measurements: Caffeines, n-Alkanes, Fatty Acid Methyl Esters, Glycines, l-Valines, Polyethylenes, and Oils. *Anal. Chem.* **2016**, *88*, 4294–4302.

(40) Kragten, J. Calculating standard deviations and confidence intervals with a universally applicable spreadsheet technique. *Analyst* **1994**, *119*, 2161–2165.

(41) Dunn, P. J. H.; Hai, L.; Malinovsky, D.; Goenaga-Infante, H. Simple spreadsheet templates for the determination of the measurement uncertainty of stable isotope ratio delta values. *Rapid Commun. Mass Spectrom.* **2015**, *29*, 2184–2186.

(42) Hoops, S.; Sahle, S.; Gauges, R.; Lee, C.; Pahle, J.; Simus, N.; Singhal, M.; Xu, L.; Mendes, P.; Kummer, U. COPASI - a complex pathway simulator. *Bioinformatics* **2006**, *22*, 3067–3074.

(43) Eichler, D. Physikochemische Eigenschaften, Verhalten und Analytik der HCH-Isomeren. *Hexachlorcyclohexan als Schadstoff in Lebensmitteln. Verlag Chemie, Weinheim* **1983**, *1417*, 65–72.

(44) Artimo, P. et al. ExPASy: SIB Bioinformatics Resource Portal. *Nucleic Acids Res* **2012**, *40*, W597–W603.

(45) Scott, K.; Lu, X.; Cavanaugh, C.; Liu, J. Optimal methods for estimating kinetic isotope effects from different forms of the Rayleigh distillation equation 1. *Geochim. Cosmochim. Acta* **2004**, *68*, 433–442.

(46) Wijker, R. S.; Adamczyk, P.; Bolotin, J.; Paneth, P.; Hofstetter, T. B. Isotopic analysis of oxidative pollutant degradation pathways exhibiting farge H Isotope fractionation. *Environ. Sci. Technol.* **2013**, *47*, 13459–13468.

(47) Coplen, T. B. Guidelines and recommended terms for expression of stable-isotope-ratio and gas-ratio measurement results. *Rapid Commun. Mass Spectrom.* **2011**, *25*, 2538–2560.

(48) Reichert, P. Aquasim - A tool for simulation and data-analysis of aquatic systems. *Wat. Sci. Technol.* **1994**, *30*, 21–30.

(49) Dorer, C.; Höhener, P.; Hedwig, N.; Richnow, H.-H.; Vogt, C. Rayleigh-based concept to

tackle strong hydrogen fractionation in dual isotope analysis - The example of ethylbenzene degradation by *Aromatoleum aromaticum*. *Environ. Sci. Technol.* **2014**, *48*, 5788–5797.

(50) Shrivastava, N.; Macwan, A. S.; Kohler, H.-P. E.; Kumar, A. Important amino acid residues of hexachlorocyclohexane dehydrochlorinases (LinA) for enantioselective transformation of hexachlorocyclohexane isomers. *Biodegradation* **2017**, *28*, 171–180.

(51) Elsner, M.; McKelvie, J.; Lacrampe-Couloume, G.; Sherwood Lollar, B. Insight into methyl *tert*-butyl ether (MTBE) stable isotope fractionation from abiotic reference experiments. *Environ. Sci. Technol.* **2007**, *41*, 5693–5700.

(52) Melander, L.; Saunders, W. H. *Reaction Rates of Isotopic Molecules*; 331 pp; John Wiley & Sons; Wiley Interscience Publication, 1980.

(53) Jia, Z. S.; Rudzinski, J.; Paneth, P.; Thibblin, A. Borderline between E1cB and E2 mechanisms. Chlorine isotope effects in base-promoted elimination reactions. *J. Org. Chem.* **2002**, *67*, 177–181.

(54) Brown, K. C.; Romano, F. J.; Saunders Jr, W. H. Mechanisms of elimination-reactions. 34. Deuterium and nitrogen isotope effects and hammett correlations in the reaction of (2-arylethyl)trimethylammonium ions with hydroxide ion in mixtures of water and dimethylsulfoxide. *J. Org. Chem.* **1981**, *46*, 4242–4246.

(55) Saunders Jr, W. H.; Edison, D. H. Mechanisms of elimination reactions. IV. Deuterium isotope effects in E2 reactions of some 2-phenylethyl derivatives. *J. Am. Chem. Soc.* **1960**, *82*, 138–142.

(56) Szatkowski, L.; Manna, R. N.; Grzybkowska, A.; Kamiński, R.; Dybala-Defratyka, A.; Paneth, P. M. Measurement and prediction of chlorine kinetic isotope effects in enzymatic systems. In *Measurement and Analysis of Kinetic Isotope Effects*; Harris, M. E., Anderson, V. E., Eds.; Methods in Enzymology; Academic Press, 2017; Vol. 596; pp 179–215.

(57) Manna, R. N.; Zinovjev, K.; Tuñòn, I.; Dybala-Defratyka, A. Dehydrochlorination of hexachlorocyclohexanes catalyzed by the LinA dehydrohalogenase. A QM/MM study. *J. Phys. Chem. B* **2015**, *119*, 15100–15109.

(58) Brittain, D. R. B.; Pandey, R.; Kumari, K.; Sharma, P.; Pandey, G.; Lal, R.; Coote, M. L.; Oakeshott, J. G.; Jackson, C. J. Competing S_N2 and E2 reaction pathways for hexachlorocyclohexane degradation in the gas phase, solution and enzymes. *Chem. Commun.* **2011**, *47*, 976–978.

(59) Ehrl, B. N.; Gharasoo, M.; Elsner, M. Isotope fractionation pinpoints membrane permeability as a barrier to atrazine biodegradation in gram-negative *Polaromonas* sp. Nea-C. *Environ. Sci. Technol.* **2018**, *52*, 4137–4144.

(60) Renpenning, J.; Rapp, I.; Nijenhuis, I. Substrate hydrophobicity and cell composition influence the extent of rate limitation and masking of isotope fractionation during microbial reductive dehalogenation of chlorinated ethenes. *Environ. Sci. Technol.* **2015**, *49*, 4293–4301.

(61) Endo, R.; Ohtsubo, Y.; Tsuda, M.; Nagata, Y. Identification and characterization of genes encoding a putative ABC-type transporter essential for utilization of γ-hexachlorocyclohexane in *Sphingobium japonicum* UT26. *J. Bacteriol.* **2007**, *189*, 3712–3720.

Graphical TOC Entry